Spatial Statistics 23 (2018) 17–35

Contents lists available at ScienceDirect

Spatial Statistics

journal homepage: www.elsevier.com/locate/spasta

Distance function modeling in optimally locating additional boreholes

Mohammad Safa, Saeed Soltani-Mohammadi *

Department of Mining Engineering, University of Kashan, Ravand Street, P.O. BOX: 87317-51167, Kashan, Iran

HIGHLIGHTS

- Using distance function reduces the calculation time.
- A new algorithm for locating the additional boreholes is presented.
- The algorithm is validated based on the Angouran mineral deposit.

ARTICLE INFO

Article history:
Received 13 November 2016
Accepted 6 November 2017
Available online 26 November 2017

Keywords:
Distance function
Additional drilling
Particle swarm optimization
Geostatistics
Combined variance

ABSTRACT

The optimal locating of additional boreholes is complicated and very time consuming. Some methods such as metaheuristic algorithms, calculation parallelism, and reducing the time of objective function calculation could be used to increase the calculation speed; among these methods, the latter is preferred due to its extensive influence on the optimization of time. The main reasons that make the objective function calculation cumbersome are mentioned hereafter, and according to their priority: (1) excessive quantity of blocks in the geological block model, and (2) inverting the matrix of average semivariogram between samples is a time consuming operation. The present study aims to decrease the calculation time by reducing the number of blocks without considering their size increment that affects accuracy. To achieve this purpose, the objective function is calculated according to the block model of uncertainty zone, which is defined by using the recently introduced distance function to investigate uncertainty in mineralized domain boundaries. In order to evaluate the performance of the present approach on reducing the calculation time as well as the precision in locating additional boreholes,

* Corresponding author.
E-mail address: saeedsoltani@kashanu.ac.ir (S. Soltani-Mohammadi).

https://doi.org/10.1016/j.spasta.2017.11.001

the results from particle swarm optimization as a metaheuristic algorithm are compared by considering two different scenarios of combined variance reduction on the basis of a three-dimensional geological block model and an uncertainty block model. The comparative results show that using the uncertainty block model reduces the calculation time by one-third, and the proposed locations of the boreholes are more consistent to the study's aim, which is to reduce the boundary's uncertainty.

1. Introduction

The 3D geological block model is utilized as a tool to illustrate the information collected from mineral deposits, and it is one of the main input parameters for various operations in mining projects such as feasibility study, planning, scheduling, etc. Mineral deposits are usually relatively heterogeneous mediums, and so their geological block models should be constructed based on the grade spatial continuity and by considering geological features such as their petrology, mineralogy and metamorphism (Duke and Hanna, 2001; Ortiz, 2006). Due to the limited number of samples collected from deposits, the geological model is tainted by uncertainty (Yamamoto et al., 2014). The uncertainty is known as a source of risk in the future phases of mine planning and decision making (Dimitrakopoulos, 1998). The uncertainty of geological modeling could be sorted into three categories: (1) uncertainty in boundary delineation, (2) uncertainty of interpolation inside the data range and extrapolation beyond the data range, and (3) lack of knowledge about underground structures such as the existence of faults (Mann, 1993).

The grade reduction in deposit boundaries follows a gentle trend that makes the exact delineation of boundaries impossible (Tercan, 1998). Defining the boundary's type requires extensive research and collection of data relevant to grade variation, rock type and geological facies (McLennan, 2008). Generally, it can be stated that two kinds of problems arise without the full and extensive sampling from boundary zone: first, the amount of overestimation in deposits geological extension is much more than expected, and second, the estimated values may lie in a range that is not logical from a geological viewpoint (Pawlowsky et al., 1993). The first problem can be usually solved by defining the boundary with a value less or greater than a predetermined value, while the second problem remains, and its impact could be noticed in several maps in which the contours are not closed lines in the marginal areas that then suddenly intersect with the boundary. To overcome these problems, geostatistical methods such as indicator kriging (Larrondo and Deutsch, 2005), probability kriging (Tercan, 1998) and geostatistical simulation (Dohm, 2003) could be utilized to evaluate the uncertainty in geological boundaries and improve the geological boundary delineation techniques.

Uncertainty reduction obligates increment of data quantity, which means additional drilling. Increasing the number of samples does not always lead to reduction in uncertainty, and it depends to a great extent on the locations of new samples (Yamamoto et al., 2014). Therefore, many researches have focused on optimizing the number of additional boreholes (Soltani-Mohammadi and Safa, 2015; Szidarovszky, 1983) and locating additional boreholes (Hossein Morshedy and Memarian, 2015; Scheck and Chou, 1983; Walton and Kauffman, 1982). Preliminary studies on the optimization of exploratory drilling pattern have been carried out manually in a two dimensional space and usually by means of an objective function defined on the basis of the kriging variance (Kim et al., 1977; Walton and Kauffman, 1982). Although the result of this method is preferable to making use of experts' experiences for locating drill holes, the simplification of the procedure by 2D assumption is considered as its drawback because the 3D effects of the grade and thickness variations are not accounted for in this assumption. Soltani and Hezarkhani (2009) solved the optimal locating problem in 3D space, but this improvement caused an increase in the calculation time (Soltani and Hezarkhani, 2009). Recently, researchers have made improvements in reducing the calculation time in 3D cases through the utilization of different metaheuristic optimization algorithms such as simulated annealing, partial swarm optimization and genetic algorithm (Cheng, 2016; Dali and Bouamama, 2015; Lee, 1997; Roeva

et al., 2013; Soltani-Mohammadi et al., 2016). Setting a limit for the solution space could be an alternative approach to reduce the calculation time. The concept of the proposed alternative is based on the calculation of objective function for a limited number of blocks, which according to the drilling objectives are more important than the others. In situations where the drilling objective improves the domain accuracy, the distance function concept could help in distinguishing and separating blocks with greater level of importance (uncertainty zone). The definition of the distance function is related to the notion of distance to an interface separating two distinct domains within which two different stationary random functions would be subsequently developed for geostatistical modeling (Hosseini, 2009). This paper tries to study the feasibility of this approach, and to monitor its impact on reducing the calculation time as well as the results of the algorithm.

2. Materials and methods

2.1. Distance function

The distance function is known as a proper method for defining both the boundary locations and the boundary's uncertainty zone due to its simplicity and flexibility (Hosseini, 2009; McLennan, 2008). The distance function can be described as the nearest Euclidean distance between two samples from two different domains or domains with different conditions such as mineralized and surrounding waste rocks domains. The value of the distance function can be positive or negative depending on whether the sample is located outside or inside the area, respectively. The distance function value increases with the sample location distance from the boundaries. This increment complies for both interior and exterior samples. The first requirement for using the distance function is to control all the data according to their sample positions, i.e. if they are located inside or outside the predetermined domain. In other words, converting data to indicator variable as follows:

$$i\left(u_\alpha\right) = \begin{cases} 1 & \text{if domain of interest present at } u_\alpha, \\ 0 & \text{otherwise}, \end{cases} \quad \alpha = 1, \ldots, n \tag{1}$$

where u is a location vector, α is the sample index and n is the number of data. The distance function is calculated for each sample based on the Euclidean distance equation with respect to the nearest sample location that possesses the opposite condition. On the other hand, for a typical sample, u_α, the nearest sample from the opposite area, $u_{\acute{\alpha}}$, is determined in such a way that $u_\alpha \neq u_{\acute{\alpha}}$, and their distance vector is the distance function value in location u_α and equals df. The numerical value of distance function could be calculated as follows (Munroe and Deutsch, 2008a):

$$df\left(u_\alpha\right) = \sqrt{\left(\frac{dx}{hx}\right)^2 + \left(\frac{dy}{hy}\right)^2 + \left(\frac{dz}{hz}\right)^2} \tag{2}$$

where dx, dy and dz represent the distance between the sample locations in x, y and z directions, respectively. hx, hy and hz are the variogram ranges in x, y and z directions, respectively. The distance function sign is also set according to its positioning in different domains, and could be determined based on the following equation:

$$df\left(u_\alpha\right) = \begin{cases} +\left(u_\alpha - u_{\acute{\alpha}}\right) & \text{if } i\left(u_\alpha\right) = 0 \\ -\left(u_\alpha - u_{\acute{\alpha}}\right) & \text{if } i\left(u_\alpha\right) = 1. \end{cases} \tag{3}$$

In the following steps, linear estimators (such as inverse distance weighing, kriging, etc.) could be used for the interpolation of the value of distance function in a regular grid (Wilde and Deutsch, 2012). Accordingly, the domain boundaries can be drawn schematically by using a zero line that is produced by connecting a set of points in which the value of distance function is zero.

The problems with applying the distance function method are that it requires a great amount of data as well as its disability to directly determine the uncertainty (Wilde and Deutsch, 2012). Deutsch and Munroe proposed the use of the C parameter for investigating the width of the uncertainty zone

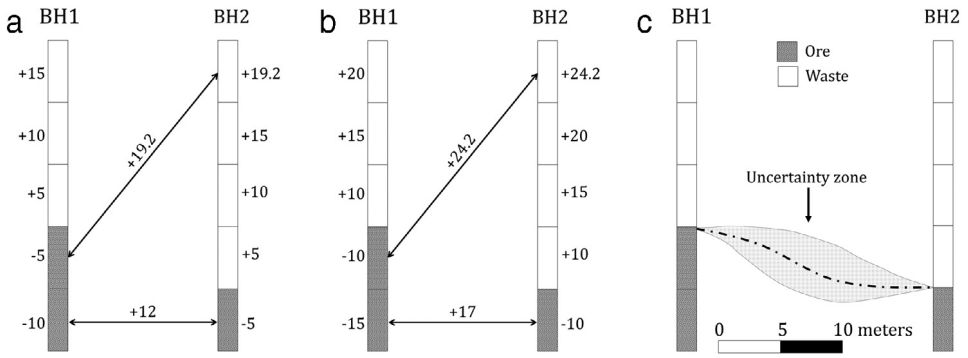

Fig. 1. Distance function variation: (a) $C = 0$, (b) $C = 5$ and (c) changes of uncertainty zone between boreholes.

in relation to the boundaries (Munroe and Deutsch, 2008a, b). C is a positive correction parameter that modifies the distance function value in all points through the following equation:

$$\hat{df}\,(u_\alpha) = \begin{cases} df\,(u_\alpha) + C & if\ i\,(u_\alpha) = 0 \\ df\,(u_\alpha) - C & if\ i\,(u_\alpha) = 1 \end{cases} \tag{4}$$

where $\hat{df}\,(u_\alpha)$ is the modified distance function. The C parameter causes an increase between the positive and negative values. Thus, the value of distance function is estimated in an ordered grid, and according to the modified distance function for the sampling points. Later, the grid points in which the value of the modified distance function is less than $-C$ are considered inside the domain, while if the function produces a value greater than C, the point is defined as being outside the domain. If the value of the modified distance function falls within a range of $-C$ to C, the point is defined as the boundary uncertainty zone. The zero line is always located within the uncertainty zone. In Fig. 1a, b, the numerical changes in the distance function are shown before ($C = 0$) and after the addition of $C = 5$ between two boreholes. The changes in the uncertainty zone for a vertical section between two boreholes are also depicted in Fig. 1c. As the figure indicates, the thickness of the uncertainty zone is zero at boreholes locations, and grows with the increasing distance from the boreholes. The extent of the boundary's uncertainty zone increases with higher values of C. Since this increase is acceptable to a certain extent, C needs to be calibrated using a proper method.

The calibration of C is accomplished by randomly splitting the data into an interpolation set and a validation set. The first category is applied for the interpolation and the calibration, while the second category is utilized for the validation (Munroe and Deutsch, 2008b). When $C = 0$, the number of misclassified data is considered as the basic mode. In the review of states when $C > 0$, the points that are located in the uncertainty zone as their distance function value lies between $-C$ and C are not accounted for because of having an unknown condition. The increase of C causes the expansion of the uncertainty zone so that a larger amount of misclassified validation data falls within this area. The calibration of C continues until the ratio of misclassified to correctly classified data reaches a desired level (Wilde and Deutsch, 2012).

2.2. Objective function

In most of the proposed algorithms for optimal locating of additional samples, the objective function is defined on the basis of the minimization of the mean kriging variance (Soltani-Mohammadi et al., 2012; Szidarovszky, 1983). The kriging variance of a block v can be determined by using the surrounding information as follows (Webster and Oliver, 2001):

$$\sigma^2_{kv} = \sum_{i=1}^{n} \lambda_i \overline{\gamma}\,(x_i - v) + \mu - \overline{\gamma}(v, v) \tag{5}$$

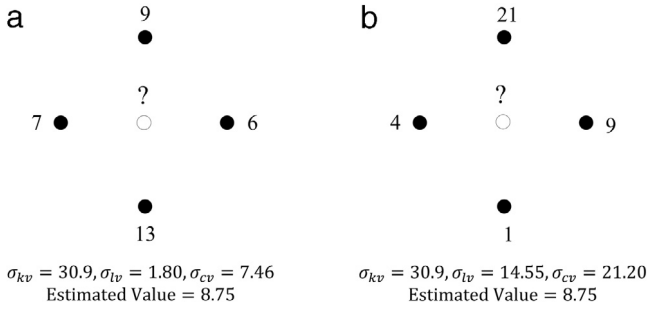

Fig. 2. Two different configurations of grade value (black circles) around an estimated point (white circle). (σ_{kv}—kriging variance, σ_{lv}—local variance, σ_{cv}—combined variance).

where n is the number of samples used for the estimation, x_i is the location of the samples, $\overline{\gamma}(x_i - v)$ is the semivariogram associated with distance $(x_i - v)$, $\overline{\gamma}(v, v)$ is the average of the semivariogram values of all the possible paired points within block v, λ_i is the kriging weight, and μ is the Lagrange multiplier. One feature of the kriging variance is that it depends on the location of samples, semivariogram parameters, and block dimension, but is independent of the grade value of samples (Journel and Huijbregts, 1978). This feature is considered as a positive and a negative property at the same time. On one hand, the value of kriging variance can be updated according to its location before drilling additional boreholes, and then the effects of drilling new boreholes are investigated (Deutsch, 1996). On the other hand, the kriging variance is not sensitive to local variability (Goovaerts, 1997) whereas natural phenomena are not homogeneous, which means that local variability should be evaluated appropriately in order to have a correct understanding about uncertainty (Yamamoto, 2000). This issue could be discussed through a simple example. In Fig. 2, two different configurations of grade values are shown around an unsampled point. The kriging variance (σ_{kv}) is the same for both configurations according to the constant state of the variogram model (a spherical model with a range of 200 m, a sill value of 100, and nugget effect of zero) and the sample locations around the estimated point. The local variability in Fig. 2b is more than that in Fig. 2a.

One of the alternatives that have been proposed to the kriging variance is the combined variance σ_{cv}^2, which is a combination of the kriging variance and the local variance σ_{lv}^2 (Arik, 1999a, b; Heuvelink and Pebesma, 2002):

$$\sigma_{cv}^2 = \sqrt{\sigma_{lv}^2 \times \sigma_{kv}^2}. \tag{6}$$

Local variance is defined as a weighted average of the squared difference between the estimated value in the center of the block ($i^*(x_o)$) and the sample values ($i(x_j)$) (Safa et al., 2016; Silva and Boisvert, 2014):

$$\sigma_{lv}^2 = \sum_{j=1}^{n} \lambda_j^2 \left[i(x_j) - i^*(x_o) \right]^2 \tag{7}$$

where n is the number of samples used for kriging each block. The samples being considered for individual block estimation could be determined based on the defined search volume (Marinoni, 2003; Sinclair and Blackwell, 2002). The advantage of the combined variance over the kriging variance is that in addition to the spatial configuration and grade continuity, it can provide a proper perspective on the grade quantity around the estimated block. For example, the calculated values of the combined variance from Fig. 2b are greater than that from Fig. 2a.

In order to consider the importance of local variability around the deposit boundaries in locating additional boreholes, the objective function is defined in the following form based on the

minimization of the block model total combined variance:

$$CV = \sum_{j=1}^{m} \sqrt[2]{\sigma_{lvj}^2 \times \sigma_{kvj}^2} \tag{8}$$

where σ_{kv} and σ_{lv} represent the kriging variance and local variance for block j, and m is the number of blocks. Finally, the optimization problem of locating boreholes is defined as follows:

$$\begin{aligned} &Min\ CV \\ &\quad Subject\ to: \\ &\qquad x_{p+q} \in D \subset R^2, q = 1, \ldots, k \end{aligned} \tag{9}$$

where p and k are the numbers of initial and additional boreholes, respectively.

After the addition of new boreholes, their sample values are required to update the objective function for each iteration of the algorithm, but acquiring such information is impossible before exploratory drilling and sample analysis. Thus, during the computation of the objective function, the local variance is calculated only once based on the existing initial information, while the kriging variance could be updated according to the proposed locations of boreholes in each iteration. In other words, the local variance is used as a weighting factor in the objective function. The utilization of this weighting factor will result in the reduction of the kriging variance so as to be more effective in the decrease of the objective function in blocks with greater local variance. The greater the local variance, the larger is the local variability, which means the objective function suggests locations for additional boreholes in areas where local variability is greater.

2.3. Particle swarm optimization (PSO)

The increase of problem extension alongside increasing the number of variables means that using conventional methods to find the optimal solution is computably impossible due to the vast extent of the problem and the complexity of calculations. For such a situation, using metaheuristic algorithms that approach faster towards the optimized solution by surveying a limited number of feasible configurations seems to be appropriate. In these algorithms, despite the exact methods of optimization, the aim is to find points as close as possible to the global optimized pattern that properly satisfies decision makers. Many metaheuristic methods have been proposed so far on the basis of the existing orders originating from natural organisms; among these methods, genetic algorithm, simulated annealing, Tabu Search and PSO are reported to be widely used (Alves da Silva and Falcão, 2007).

PSO is a stochastic evolutionary computation technique that is used for optimization problems (Eberhart and Kennedy, 1995; Fukuyama, 2007). This algorithm is an inspiration for some unique social behavior of natural beings such as group formation of birds and fish for movement, and has a rational and economically feasible calculation process from the viewpoint of required memory as well as computational speed (Eberhart and Kennedy, 1995). PSO algorithm owns a memory capable of recording the knowledge of proper solutions in all particles. In other words, in PSO, each social member changes its own location according to individual and social experiences. These advantages make the selection of PSO preferable for the optimization of locating boreholes. Till now, PSO has been utilized to find the optimized solutions for a range of similar problems like the optimal locating of additional boreholes (Soltani-Mohammadi et al., 2016), the optimized locating of petroleum wells (Ding et al., 2014; Onwunalu and Durlofsky, 2010), improving the production planning of open pit mines (Ferland et al., 2007; Khan and Niemann-Delius, 2014, 2015), safety studies in mining projects (Meng et al., 2012; Wang et al., 2015), monitoring of blasting impacts in mines (Hajihassani et al., 2014), and slope stability (Cheng et al., 2007). Inertia weight, personal learning coefficient, global learning coefficient as well as population size (swarm size) can be mentioned among the most dominant parameters of the PSO algorithm. Fig. 3 illustrates a flowchart of the proposed PSO-based algorithm.

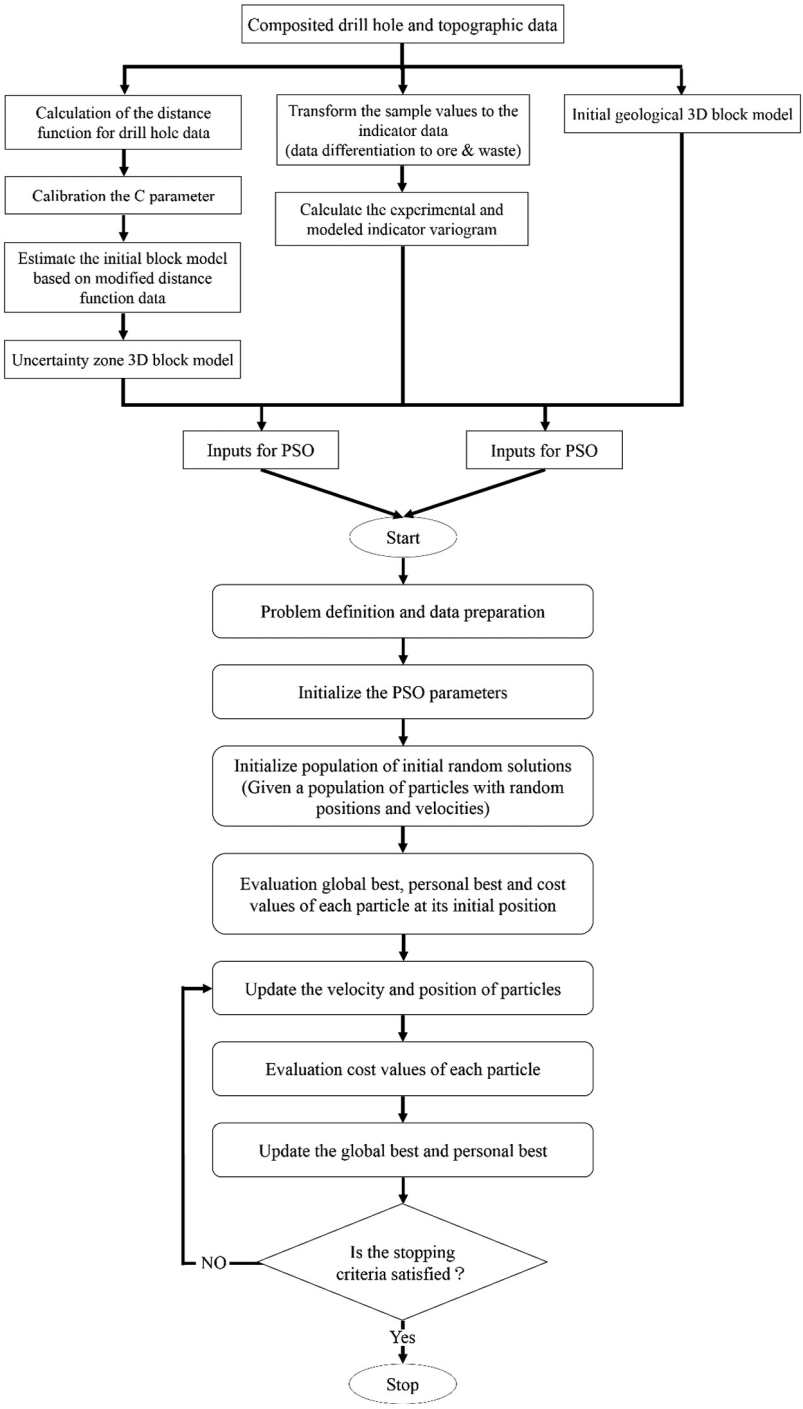

Fig. 3. Flowchart of the PSO-based proposed algorithm.

3. Case study

In order to monitor the performance of the proposed algorithm, a case study of locating additional boreholes in Angouran mineral deposits has been investigated. Angouran is one of the most important carbonate-sulfide zinc and lead deposits that is located in northwest Iran (Fig. 4a). The deposits are formed within a neoproterozoic metamorphic complex that mostly consists of marble and schist (Gilg et al., 2003).

The input parameters of the proposed algorithm for locating additional boreholes to minimize the uncertainty in boundaries are: (1) the positions of initial boreholes and their samples values, (2) the threshold grade, (3) the parameters of the indicator variogram model, (4) the 3D block model of the deposits, (5) the 3D block model of the uncertainty zone, (6) the key parameters of the PSO algorithm, and (7) the number of additional boreholes. All the additional boreholes are designed to be vertical considering the topographical conditions and the 3D extension of the ore body.

From 42 initial exploratory boreholes, a total core length of 4120 m was sampled. The distribution map of the initial boreholes is presented in Fig. 4b. The objective of the spatial sampling was to survey the ore body characteristics such as shape, grade variation, etc. Purposive sampling design was used for planning the drilling pattern. The constraint modeling procedure and the indicator kriging estimator were used for 3D modeling of the ore body and zinc grade, respectively. Considering the cut-off grade value of 3% for zinc, 1210 m of core samples had intersected the ore body. After the transformation of grade data to indicator variables, the experimental indicator variogram was calculated, and a spherical model was fitted to it with range, sill and nugget effect of 125 m, 0.203, and 0.035, respectively (Fig. 5).

The 3D geological model was produced according to 12 vertical sections with a scale of 1:500, a topographical map with a scale of 1:1000, and data derived from the sampling of 42 initial boreholes, which were then converted into a 3D block model, including 1662 blocks with dimensions of $20 \times 20 \times 10$ m.

The spatial stratified heterogeneity of data was measured by q-statistic (Wang et al., 2016) based on the following steps:

Step 1: Since the sample was not distributed normally, the grade data was transformed by normal score transformation (Deutsch and Journel, 1992).

Step 2: The q and F statistics and non-centrality λ were calculated on the basis of the following equations:

$$\begin{aligned} q &= 1 - \frac{\sum_1^L N_i \sigma_i^2}{N\sigma^2} = 0.573 \\ F &= \frac{(N-L)}{(L-1)} \times \frac{q}{(1-q)} = 1101 \\ \lambda &= \frac{1}{\sigma^2}\left[\sum_1^L \mu_i^2 - \frac{1}{N}\left(\sum_1^L \sqrt{N_i}\mu_i\right)\right] = 1.6 \end{aligned} \tag{10}$$

where N is the number of data (824), σ^2 is the variance of normalized data (1), L is the number of domains (2), N_i is the number of samples in each domain ($N_1 = 582$, $N_2 = 242$) and σ_i^2 is the domain variance ($\sigma_1^2 = 0.497$ and $\sigma_2^2 = 0.26$) and μ_i is the domain mean ($\mu_1 = -0.487$ *and* $\mu_2 = 1.172$).

Step 3: $F_\alpha\ (L-1, N-L, \lambda)$ was calculated by running the http://keisan.casio.com/exec/system/1180573166, with cumulative mode = upper Q, cumulative distribution = 0.01, degree of freedom v1 = 1, degree of freedom v2 = 822, and non-centrality $\lambda = 1.6$. We obtained $F_\alpha\ (1, 822, 1.6) = 12.97$.

Step 4: Since $F = 1101 > 12.97 = F_\alpha\ (1, 822, 1.6)$, we concluded that the spatial stratified heterogeneity was significant (Details about the q-statistic can be found in the literature Lipsett and Campleman, 1999; Wang et al., 2016).

The blocks located on the boundary's uncertainty zone were determined by using the distance function with the aim to reduce the computational time of the objective function. These blocks influence the calculation of objective function more effectively than the other blocks with regard to the aim of the study. In order to calculate the distance function and the calibration of C, a code was

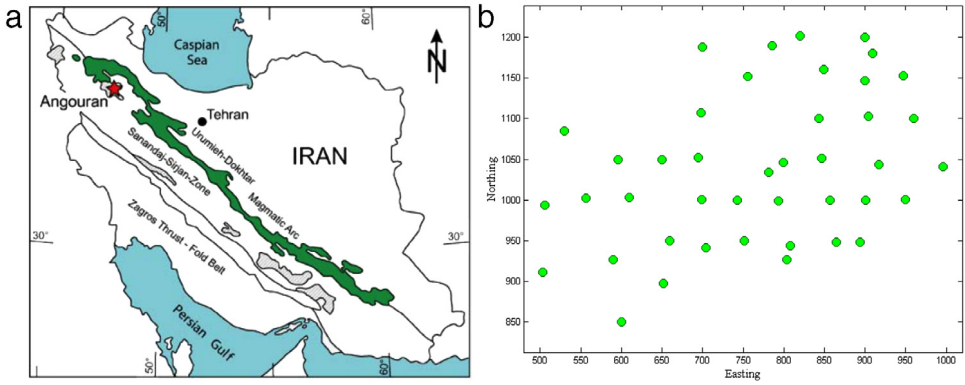

Fig. 4. (a) Location of the Angouran deposit in the Zagros orogenic belt. (b) Pattern of initial boreholes.

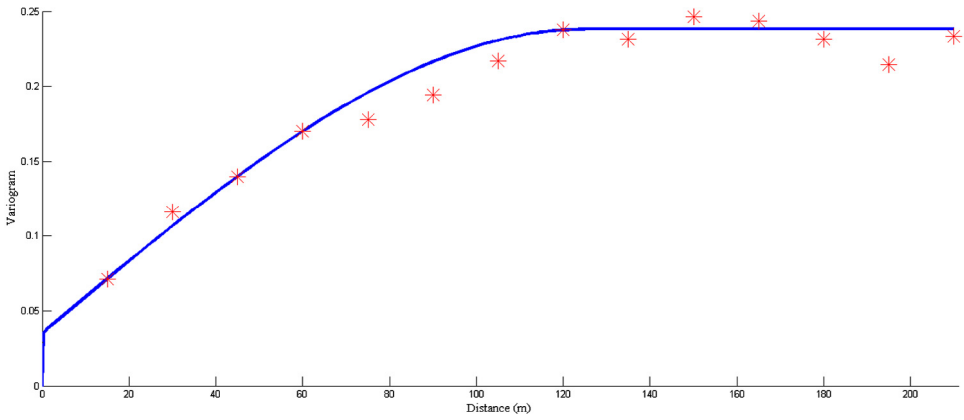

Fig. 5. Experimental indicator variogram and the fitted variogram model (a spherical model with range, sill and nugget effect of 125 m, 0.203 and 0.035, respectively).

written in MATLAB based on a proposed algorithm by Monroe and Deutsch (Munroe and Deutsch, 2008a). The input parameters of the code were: (1) the location of the initial boreholes and the grade values derived from their samples, (2) the threshold value, and (3) the 3D block model of the deposit. According to the algorithm, 90% of the data or 3708 samples were used for the distance function calculation and the remaining 412 samples were considered as validation data. As shown in Fig. 6, since $C = 12$, on one side, the primary trend of decline ended for the quantity of wrong estimations, and on the other side, despite the increase in the number of blocks located inside the uncertainty zone towards $C = 18$, the number of wrong estimations remained as 41, which led to 12 being selected as the calibrated value of C. Accordingly, as per the distance function, 504 blocks (i.e. 30.3% of the initial block model) were located in the uncertainty zone. Fig. 7 presents a histogram of the estimated values using the distance function considering $C = 12$.

In order to prove the code's efficiency, a map of the probabilities exceeding the threshold value and their uncertainty zone at elevation 2890 m is illustrated in Fig. 8a, b. The greatest value for uncertainty occurs where the estimated indicator value is 0.5, which means that the probability of occurrence of mineralized and surrounding waste rocks is equal, while the least value occurs when the estimated indicator value is 0 or 1. On the other hand, as shown in Fig. 8b, most of the blocks identified in the

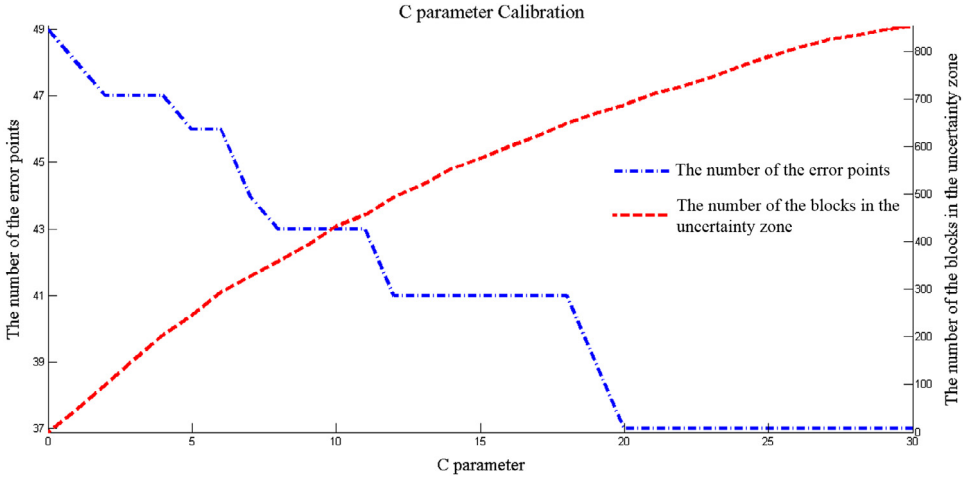

Fig. 6. Number of wrong estimations and blocks located inside the uncertainty zone versus different values of C.

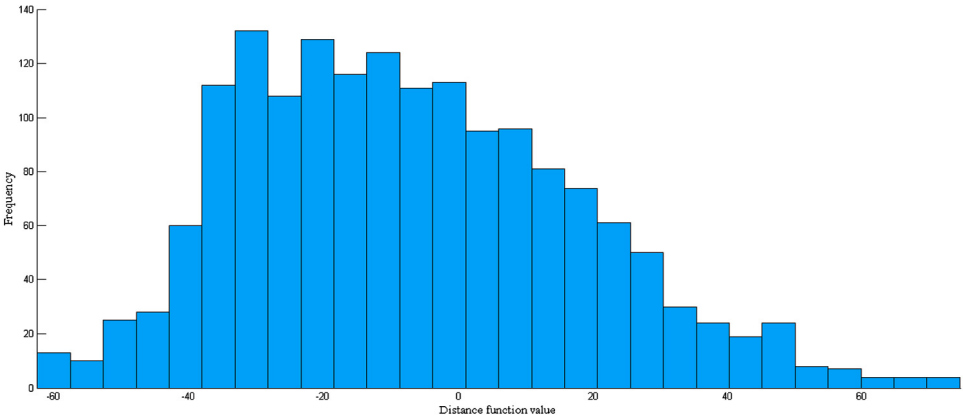

Fig. 7. Histogram showing the estimated values of distance function for $C = 12$.

uncertainty zone have index values ranging from 0.35 to 0.65, which means the proposed algorithm performs properly.

The PSO parameters were determined on the basis of the Clerc and Kennedy methods (Clerc and Kennedy, 2002). The inertia weight was set to be 0.7298, the personal and global learning coefficients were selected the same as 1.49445. To determine the optimal population size, a limited number of data derived from the initial block model at elevation 2940 m was selected and used to calculate the optimal quantity of population size through a trial and error method (Radnitzky et al., 1987) that finally resulted in the selection of 100 as the population size. This process was conducted with high level of precision to avoid having either a very great population size that could make the algorithm to get stuck during the local optimization process or, on the contrary, having a very small population size that would make it very time consuming to reach the optimal solution. Both cases are inappropriate. The stopping criterion for the algorithm is that the process should end if the objective function value does not decrease during 50 iterations.

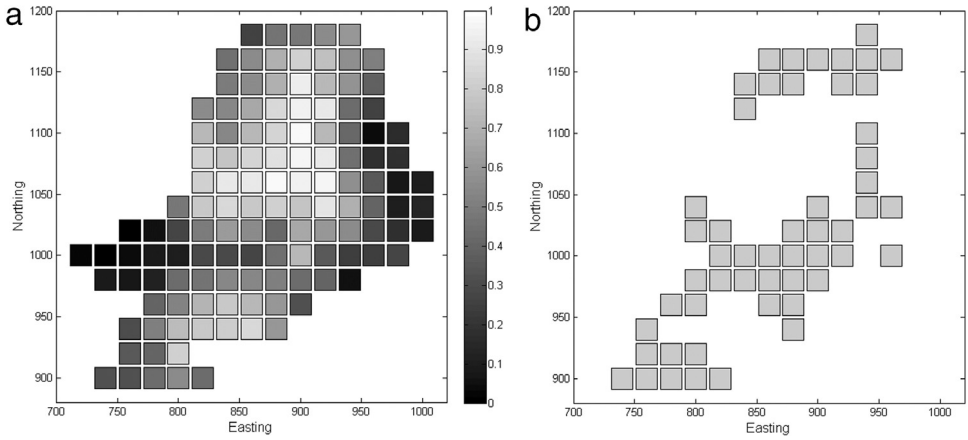

Fig. 8. Blocks at elevation 2890 m: (a) estimated indicator values, (b) uncertainty zone identified by the distance function algorithm.

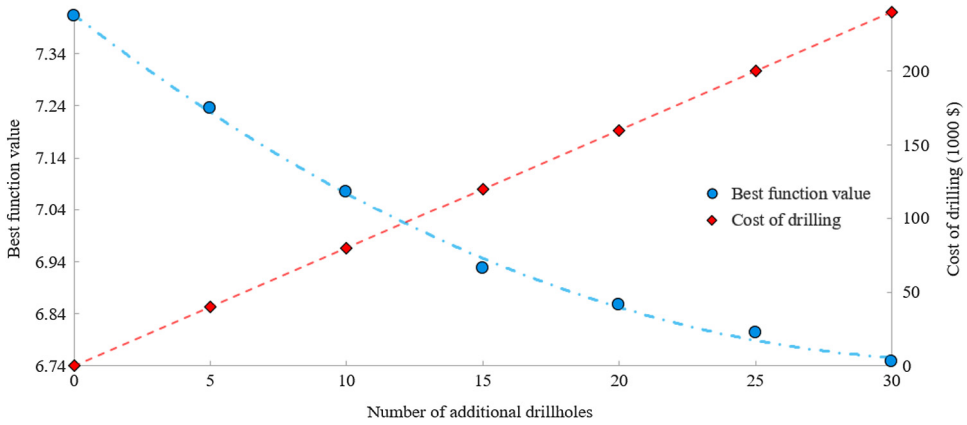

Fig. 9. Objective function and drilling cost variations versus the number of additional boreholes.

4. Results and discussion

The two main steps in designing the additional boreholes are: (1) the determination of the required number of samples to achieve the predefined goals, and (2) locating additional samples (Haldar, 2013). Maintaining a balance between the effects of adding an extra number of boreholes on the changes in the objective function and the drilling cost was utilized to determine the required quantity of additional boreholes. For this purpose, the changes resulting from drilling the number of new boreholes from 0 to 30 were evaluated with regard to drilling cost, objective function value and reduction of objective function value until 100 iterations (which is 10 000 number of function evaluation) were monitored for blocks located at an elevation of 2940 m (Fig. 9). In the present study, the average cost for drilling each borehole was defined as $40,000. As can be seen in Fig. 9, the increase in the number of additional boreholes from 0 to 15 positively affected the declining process of the objective function, but the further addition of boreholes did not seem feasible due the small changes in the objective function and increase in drilling cost.

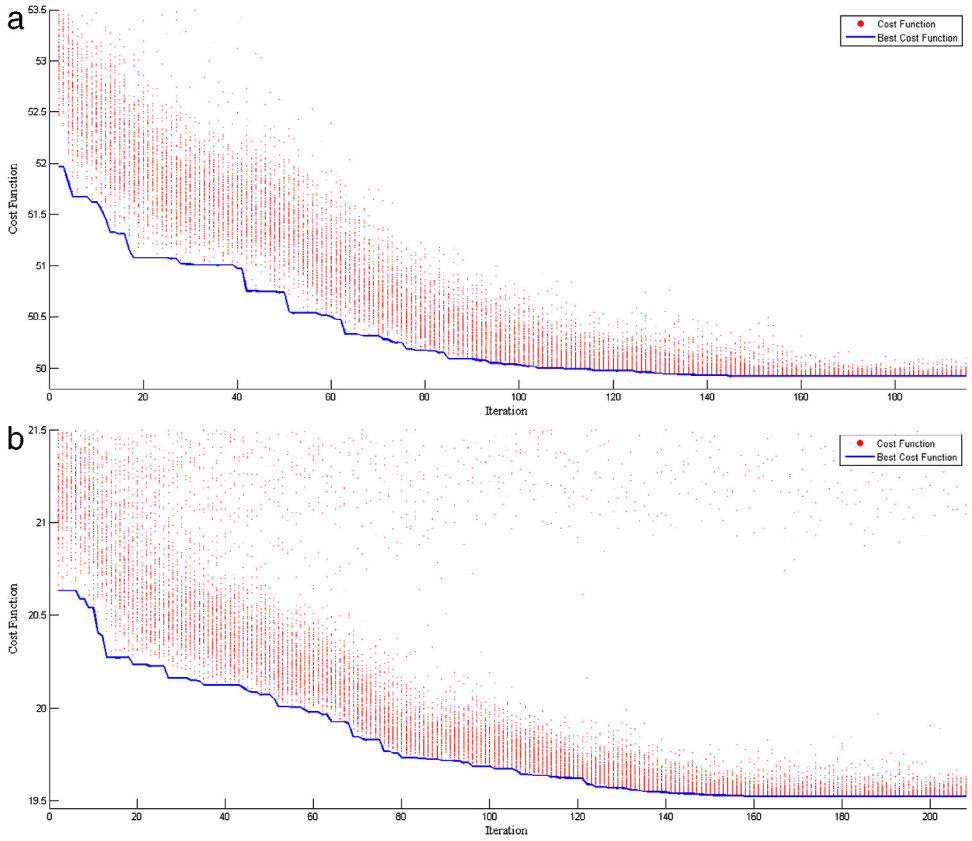

Fig. 10. Changes of objective function and its optimization process through PSO algorithm considering (a) the geological block model and (b) uncertainty zone of the block model.

To investigate the effects caused by the reduction in computational time of the objective function as a result of limiting the geological block model to the boundary's uncertainty block model, two scenarios were tried to calculate the objective function. In the first scenario, the geological block model was applied to calculate the objective function, and in the second case, the calculation was carried out by solely considering the blocks located inside the uncertainty zone. The changes in the objective function value through the optimization process on the basis of considering the geological block model and the block model of uncertainty are shown in Fig. 10a and b, respectively. As it can be seen, there was no significant difference in the optimization process between the two scenarios, but regarding the calculation time, in the first scenario, in which the geological block model was considered, each iteration that equaled 100 numbers of function evaluation took approximately 64 s and the whole process till gaining the answer took 154 min after 145 iterations, while in the second scenario, each iteration took about 20 s and the whole calculation time was reduced to 52 min after 158 iterations.

The locations of the proposed boreholes as per both the scenarios together with the initial boreholes are presented in Fig. 11. Figs. 12 and 13 provide the combined variance values for elevations 2940 m and 2970 m, respectively, according to the initial drillings and the additional boreholes proposed by the algorithm of both the scenarios. To evaluate the performance of these scenarios, their proposed boreholes locations were compared according to the boundary's uncertainty zone. As indicated in Fig. 14, although both the scenarios suggest that most of their proposed boreholes are in the same locations, the results from the second scenario are more consistent with expert opinion.

Table 1
The influence of proposed boreholes on objective function value (total combined variance) for two different scenarios.

	Geological block model			Block model of uncertainty zone		
	Initial boreholes	Initial and additional boreholes	Reduction percentage	Initial boreholes	Initial and additional boreholes	Reduction percentage
First scenario	55.04	50.14	8.9	21.52	20.01	7.0
Second scenario	55.04	51.02	7.3	21.52	19.62	8.8

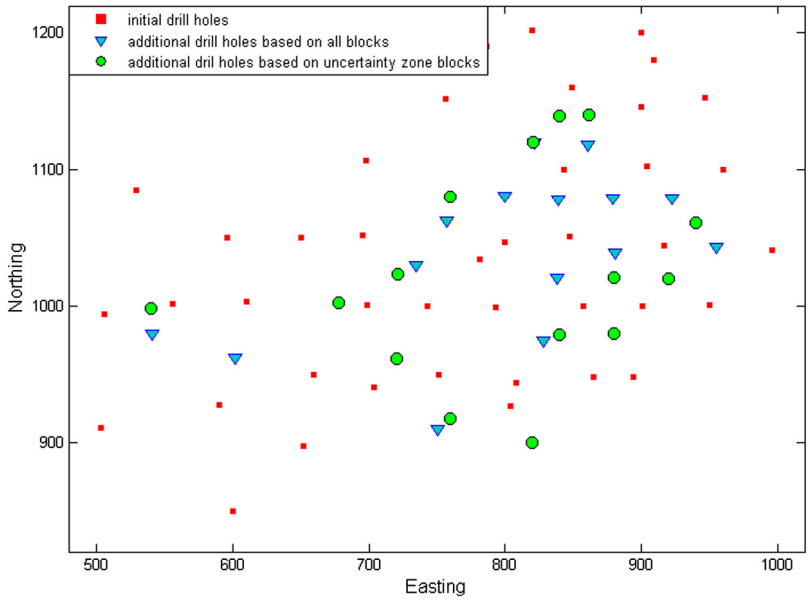

Fig. 11. Location of initial boreholes, proposed boreholes by the algorithm according to the geological block model and the block model of uncertainty zone are shown as squares, triangles and circles, respectively.

The effects of the proposed boreholes on the total combined variance for the deposit block model and uncertainty zone were also investigated. As per Table 1, the algorithm's performance in the first scenario was slightly higher (1.6%) considering the geological block model, while the second scenario demonstrated a better performance (1.8%) in the block model of uncertainty zone. Thus, it can be concluded that when the objective function is calculated based on the geological block model, a portion of the reduction of the boundary's uncertainty is located in either the mineralized or the surrounding waste rocks blocks. Since the aim of the present study was to reduce the uncertainty of deposits boundaries, the application of the second scenario is better from the viewpoint of the algorithm's performance. The comparison of the algorithm's running time for the two scenarios revealed that the calculation time was reduced to one-third when applying the second scenario.

5. Conclusions

The 3D geological model produced on the basis of the collected samples was basically fraught with uncertainties, and so the attempt was to enhance the level of our knowledge and information about deposits, in other words, to reduce the uncertainties as much as possible by drilling additional boreholes. It is known that the boundary between the mineralized and the surrounding waste rocks is the most probable area in which uncertainty occurs. The amount of effects exerted by additional boreholes depends to a great extent on their locations, so the locating process must be optimized.

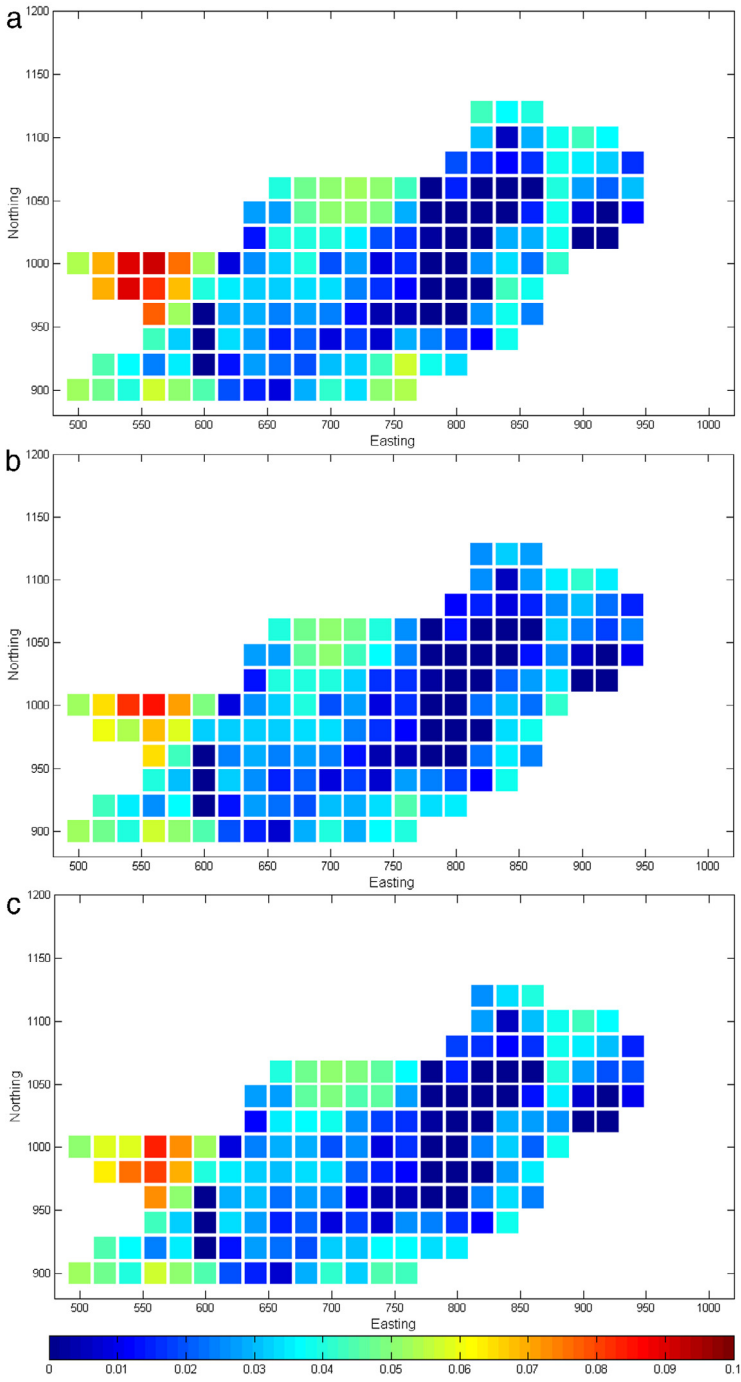

Fig. 12. Combined variance maps for elevation 2940 m, based on: (a) initial boreholes, (b) additional boreholes proposed by the algorithm for the geological block model and (c) proposed additional boreholes for uncertainty zone.

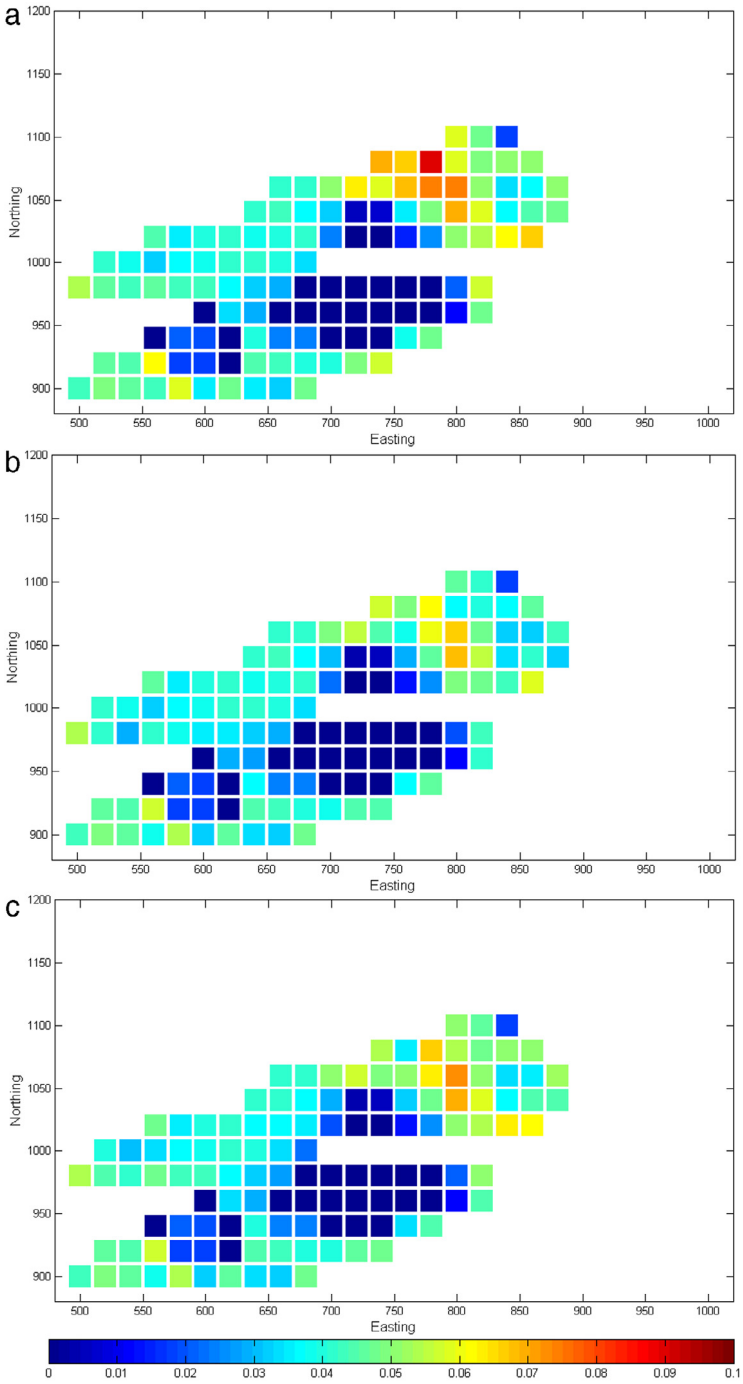

Fig. 13. Combined variance maps for elevation 2970 m, based on: (a) initial boreholes, (b) additional boreholes proposed by the algorithm for the geological block model and (c) proposed additional boreholes for uncertainty zone.

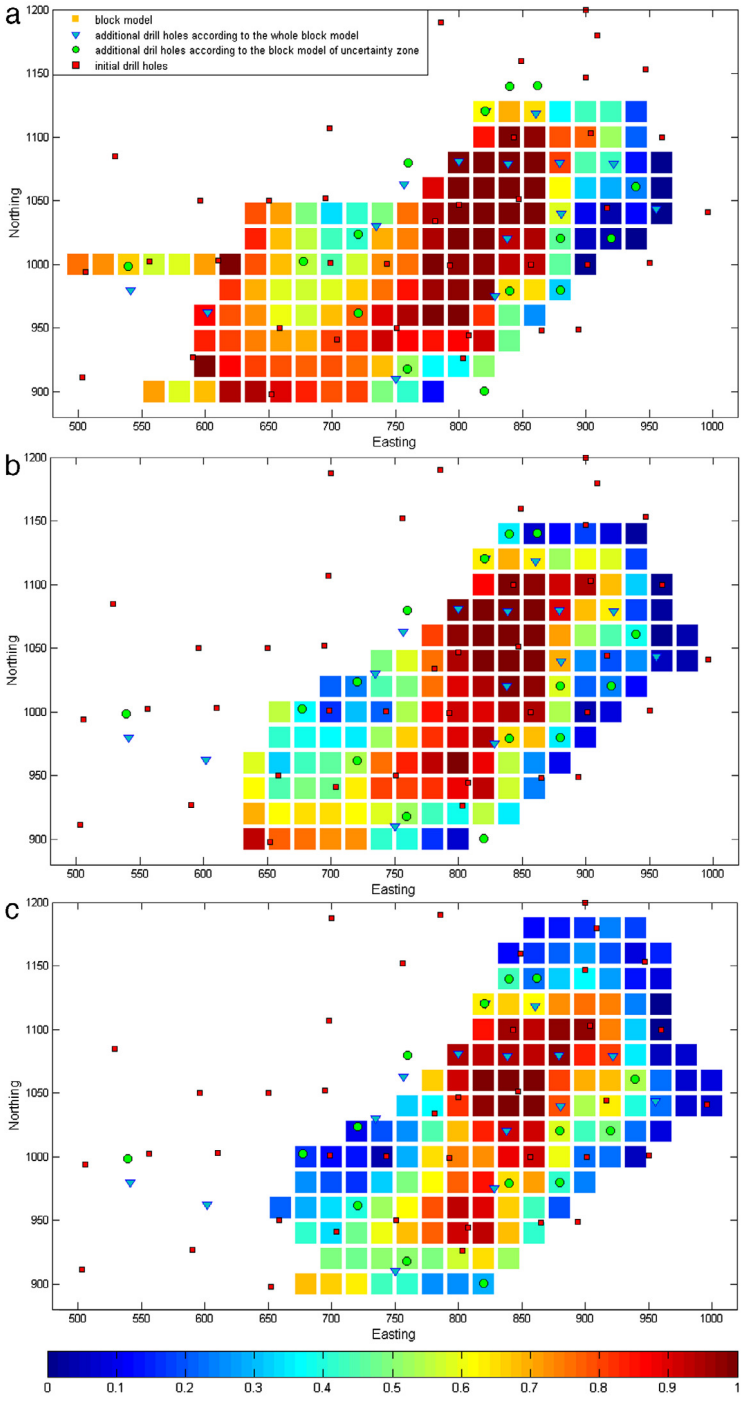

Fig. 14. Comparison of proposed locations for boreholes from the two scenarios in elevations: (a) 2930 m, (b) 2920 m and (c) 2910 m on the block model of estimated indicator values.

The optimal locating of additional boreholes is a very complex and time consuming process. Besides using metaheuristic algorithms, one solution is to shrink the target population of the calculation and try to detect it more carefully, in other words, reach the answer with less amount of calculations. In order to select the most influential blocks for the calculation process, a precise and scientific solution should be used. In the present paper, the concept of distance function was utilized to detect the uncertainty zone in deposit boundaries or in other words, reduce the quantity of blocks. In case of using the distance function, a problem is that uncertainty cannot be determined directly. Thus, by introducing the parameter C and assigning the value of 12 to it, the block model of uncertainty can be identified quantitatively after completing the calculation for calibration. By implementing this method, the number of blocks used to calculate the objective function decreased from 1662 to 504.

In order to address the two main challenges of additional drilling, after variography studies and defining the objective function, the optimization calculations were carried out based on the PSO algorithm in two steps by using the data collected from the Angouran deposits. In the first step, the changes caused by adding a number of boreholes from 0 to 30 for blocks at an elevation of 2940 m were investigated with regard to the drilling cost, the objective function value, and the objective function reduction till 100 iterations, and then the optimum number of additional boreholes was calculated to be 15. The second step of the optimization calculations was carried out according to two different scenarios of the 3D block model of the deposits and the uncertainty block model. The results revealed that the second scenario showed a better performance with respect to the algorithm's performance:

- Instead of the 3D block model of the deposits, applying the block model of uncertainty reduced the calculation time to less than one-third.
- The proposed locations for boreholes were compared to the boundary's uncertainty zone, and although both scenarios proposed the same locations for a number of additional boreholes, the results of the second scenario were more consistent with expert opinion.
- The effects of the proposed boreholes on the total combined variance of the block model of the deposits and the uncertainty zone were investigated, and it was found that when the calculations of the objective function were carried out according to the 3D block model of the deposits, a portion of the reduction of uncertainty zone was located in the interior or the exterior blocks of the mineralized domain.

Spatial autocorrelation has been the only matter of concern in all the studies concerning the locating of additional boreholes, while spatial heterogeneity (Li et al., 2008; Lin et al., 2008; Wang et al., 2009) has been omitted. It is recommended that the future studies regarding the locating of additional boreholes should use deposits in different geological zones to represent spatial stratified heterogeneity and in their case studies as well.

Acknowledgments

This work was supported by the University of Kashan (grant number 573901). The authors are indebted to the anonymous reviewers for their valuable comments on an earlier draft of this paper.

References

Alves da Silva, A.P., Falcão, D.M., 2007. Fundamentals of Genetic Algorithms, Modern Heuristic Optimization Techniques. John Wiley & Sons, Inc, pp. 25–42.

Arik, A., 1999a. An alternative approach to resource classification. In: International Symposium on Computer Applications in the Mineral Industries, APCOM'99, pp. 45–53.

Arik, A., 1999b. Uncertainty, confidence intervals and resource categorization: a combined variance approach. In: Proc. ISGSM, Perth, Australia.

Cheng, Y.M., 2016. Hybrid metaheuristic algorithms in geotechnical engineering. In: Yang, X.-S., Bekdaş, G., Nigdeli, S.M. (Eds.), Metaheuristics and Optimization in Civil Engineering. Springer International Publishing, Cham, pp. 277–302.

Cheng, Y.M., Li, L., Chi, S.-c., Wei, W.B., 2007. Particle swarm optimization algorithm for the location of the critical non-circular failure surface in two-dimensional slope stability analysis. Comput. Geotech. 34, 92–103.

Clerc, M., Kennedy, J., 2002. The particle swarm-explosion, stability, and convergence in a multidimensional complex space. IEEE Trans. Evol. Comput. 6, 58–73.

Dali, N., Bouamama, S., 2015. gpu-pso: Parallel particle swarm optimization approaches on graphical processing unit for constraint reasoning: Case of max-csps. Procedia Comput. Sci. 60, 1070–1080.
Deutsch, C.V., 1996. Correcting for negative weights in ordinary kriging. Comput. Geosci. 22, 765–773.
Deutsch, C.V., Journel, A.G., 1992. GSLIB: Geostatistical Software Library and User's Guide. Oxford University Press.
Dimitrakopoulos, R., 1998. Conditional simulation algorithms for modelling orebody uncertainty in open pit optimisation. Int. J. Surf. Min. Reclam. Environ. 12, 173–179.
Ding, S., Jiang, H., Li, J., Tang, G., 2014. Optimization of well placement by combination of a modified particle swarm optimization algorithm and quality map method. Comput. Geosci. 18, 747–762.
Dohm, C., 2003. Application of simulation techniques for combined risk assessment of both geological and grade models–an example. In: 2003 APCOM Proceedings. SAIMM, Cape Town, pp. 351-354.
Duke, J., Hanna, P., 2001. Geological interpretation for resource modelling and estimation. Mineral Resource and Ore Reserve Estimation–The AusIMM Guide to Good Practice, The Australasian Institute of Mining and Metallurgy: Melbourne. pp. 147–156.
Eberhart, R., Kennedy, J., 1995. A new optimizer using particle swarm theory. In: Proceedings of the Sixth International Symposium on Micro Machine and Human Science, 1995. MHS'95., pp. 39–43.
Ferland, J., Amaya, J., Djuimo, M., 2007. Application of a particle swarm algorithm to the capacitated open pit mining problem. In: Mukhopadhyay, S., Gupta, G. (Eds.), Autonomous Robots and Agents. Springer, Berlin Heidelberg, pp. 127–133.
Fukuyama, Y., 2007. Fundamentals of Particle Swarm Optimization Techniques, Modern Heuristic Optimization Techniques. John Wiley & Sons, Inc, pp. 71–87.
Gilg, H., Allen, C., Balassone, G., Boni, M., Moore, F., 2003. The 3-stage evolution of the Angouran Zn ''oxide''-sulfide deposit, Iran. In: Mineral Exploration and Sustainable Development. Millpress, Rotterdam, pp. 77–80.
Goovaerts, P., 1997. Geostatistics for Natural Resources Evaluation. Oxford University Press.
Hajihassani, M., Jahed Armaghani, D., Sohaei, H., Tonnizam Mohamad, E., Marto, A., 2014. Prediction of airblast-overpressure induced by blasting using a hybrid artificial neural network and particle swarm optimization. Appl. Acoust. 80, 57–67.
Haldar, S.K., 2013. Mineral Exploration Principles and Applications. Elsevier, Waltham, Mass.
Heuvelink, G.B., Pebesma, E.J., 2002. Is the ordinary kriging variance a proper measure of interpolation error. In: The Fifth International Symposium on Spatial Accuracy Assessment in Natural Resources and Environmental Sciences. RMIT University, Melbourne, pp. 179–186.
Hossein Morshedy, A., Memarian, H., 2015. A novel algorithm for designing the layout of additional boreholes. Ore Geol. Rev. 67, 34–42.
Hosseini, A.H., 2009. Probabilistic Modeling of Natural Attenuation of Petroleum Hydrocarbons. University of Alberta, p. 359.
Journel, A.G., Huijbregts, C.J., 1978. Mining Geostatistics. Academic Press, London ; New York.
Khan, A., Niemann-Delius, C., 2014. Production scheduling of open pit mines using particle swarm optimization algorithm. Adv. Oper. Res. 2014, 9.
Khan, A., Niemann-Delius, C., 2015. Application of particle swarm optimization to the open pit mine scheduling problem. In: Niemann-Delius, C. (Ed.), Proceedings of the 12th International Symposium Continuous Surface Mining - Aachen 2014. Springer International Publishing, pp. 195–212.
Kim, Y., Myers, D.E., Knudsen, H., 1977. Advanced Geostatistics in Ore Reserve Estimation and Mine Planning: US Department of Energy. Grand Junction, Colorado.
Larrondo, P., Deutsch, C., 2005. Accounting for geological boundaries in geostatical modeling of multiple rock types. In: Leuangthong, O., Deutsch, C. (Eds.), Geostatistics Banff 2004. Springer, Netherlands, pp. 3–12.
Lee, D., 1997. Multiobjective design of a marine vehicle with aid of design knowledge. Internat. J. Numer. Methods Engrg. 40, 2665–2677.
Li, L., Wang, J., Cao, Z., Zhong, E., 2008. An information-fusion method to identify pattern of spatial heterogeneity for improving the accuracy of estimation. Stoch. Environ. Res. Risk Assess. 22, 689–704.
Lin, Y.-P., Yeh, M.-S., Deng, D.-P., Wang, Y.-C., 2008. Geostatistical approaches and optimal additional sampling schemes for spatial patterns and future sampling of bird diversity. Global Ecol. Biogeogr. 17, 175–188.
Lipsett, M., Campleman, S., 1999. Occupational exposure to diesel exhaust and lung cancer: a meta-analysis. Am. J. Public Health 89, 1009–1017.
Mann, C.J., 1993. Uncertainty in Geology. Computers in Geology–25 Years of Progress. Oxford University Press, Oxford, pp. 241–254.
Marinoni, O., 2003. Improving geological models using a combined ordinary–indicator kriging approach. Eng. Geol. 69, 37–45.
McLennan, J.A., 2008. The Decision of Stationarity. University of Alberta, p. 191.
Meng, Q., Ma, X., Zhou, Y., 2012. Application of the PSO-SVM model for coal mine safety assessment. In: 2012 Eighth International Conference on Natural Computation (ICNC). IEEE, pp. 393–397.
Munroe, M.J., Deutsch, C.V., 2008a. A methodology for modeling vein-type deposit tonnage uncertainty. Center for Computational Geostatistics Annual Report 10.
Munroe, M.J., Deutsch, C.V., 2008b. Full Calibration of *C* and Beta in the Framework of Vein-type Deposit Tonnage Uncertainty. University of Alberta, Center for Computational Geostatistics Annual Report 10, p. 16 pp.
Onwunalu, J., Durlofsky, L., 2010. Application of a particle swarm optimization algorithm for determining optimum well location and type. Comput. Geosci. 14, 183–198.
Ortiz, X., 2006. Geostatistical estimation of mineral resources with soft geological boundaries: a comparative study. J. South. Afr. Inst. Min. Metall. 106, 577–584.
Pawlowsky, V., Olea, R.A., Davis, J.C., 1993. Boundary assessment under uncertainty: a case study. Math. Geol. 25, 125–144.

Radnitzky, G., Bartley, W.W., Popper, K.R., 1987. Evolutionary Epistemology, Rationality, and the Sociology of Knowledge. Open Court Publishing.
Roeva, O., Fidanova, S., Paprzycki, M., 2013. Influence of the population size on the genetic algorithm performance in case of cultivation process modelling. In: 2013 Federated Conference on Computer Science and Information Systems, pp. 371–376.
Safa, M., Soltani-Mohammadi, S., Kurdi, M., 2016. Optimal design of additional sampling pattern for drinking-water quality control. Environ. Dev. Sustainabil. 1–14.
Scheck, D., Chou, D.-R., 1983. Optimum locations for exploratory drill holes. Int. J. Min. Eng. 1, 343–355.
Silva, D., Boisvert, J., 2014. Mineral resource classification: a comparison of new and existing techniques. J. South. Afr. Inst. Min. Metall. 114, 265–273.
Sinclair, A.J., Blackwell, G.H., 2002. Applied Mineral Inventory Estimation. Cambridge University Press.
Soltani, S., Hezarkhani, A., 2009. Additional exploratory boreholes optimization based on three-dimensional model of ore deposit. Arch. Min. Sci. 54, 495–506.
Soltani-Mohammadi, S., Hezarkhani, A., Tercan, A.E., 2012. Optimally locating additional drill holes in three dimensions using grade and simulated annealing. J. Geol. Soc. India 80, 700–706.
Soltani-Mohammadi, S., Safa, M., 2015. Optimally locating additional drill holes to increase the accuracy of ore/waste classification. Min. Technol. 124, 213–221.
Soltani-Mohammadi, S., Safa, M., Mokhtari, H., 2016. Comparison of particle swarm optimization and simulated annealing for locating additional boreholes considering combined variance minimization. Comput. Geosci. 95, 146–155.
Szidarovszky, F., 1983. Multiobjective observation network design for regionalized variables. Int. J. Min. Eng. 1, 331–342.
Tercan, A.E., 1998. Assessment of boundary uncertainty in a coal deposit using probability kriging. Trans.-Inst. Min. Metall. 107, A51–A54.
Walton, D., Kauffman, P., 1982. Some practical considerations in applying geostatistics to coal reserve estimation. SME-AIME, Dallas.
Wang, J.-F., Christakos, G., Hu, M.-G., 2009. Modeling spatial means of surfaces with stratified nonhomogeneity. IEEE Trans. Geosci. Remote Sens. 47, 4167–4174.
Wang, Y., Lu, C., Zuo, C., 2015. Coal mine safety production forewarning based on improved BP neural network. Int. J. Min. Sci. Technol. 25, 319–324.
Wang, J.-F., Zhang, T.-L., Fu, B.-J., 2016. A measure of spatial stratified heterogeneity. Ecol. Indic. 67, 250–256.
Webster, R., Oliver, M.A., 2001. Geostatistics for Environmental Scientists. John Wiley & Sons, Chichester, England ; New York.
Wilde, B., Deutsch, C., 2012. Kriging and simulation in presence of stationary domains: Developments in boundary modeling. In: Abrahamsen, P., Hauge, R., Kolbjørnsen, O. (Eds.), Geostatistics Oslo 2012. Springer, Netherlands, pp. 289–300.
Yamamoto, J., 2000. An alternative measure of the reliability of ordinary kriging estimates. Math. Geol. 32, 489–509.
Yamamoto, J.K., Koike, K., Kikuda, A.T., Campanha, G.A.d.C., Endlen, A., 2014. Post-processing for uncertainty reduction in computed 3D geological models. Tectonophysics 633, 232–245.